Journal of Organometallic Chemistry 734 (2013) 25–31

Contents lists available at SciVerse ScienceDirect

Journal of Organometallic Chemistry

journal homepage: www.elsevier.com/locate/jorganchem

The synthesis of biologically relevant conjugates of $Re(CO)_3$ using pyridine-2-carboxyaldehyde

Roshinee Costa [a], Kullapa Chanawanno [a], James T. Engle [a], Bertha Baroody [b], Richard S. Herrick [b,*], Christopher J. Ziegler [a,*]

[a] Department of Chemistry, University of Akron, Akron, OH 44325-3601, USA
[b] Department of Chemistry, College of the Holy Cross, Worcester, MA 01610, USA

ARTICLE INFO

Article history:
Received 22 August 2012
Received in revised form
11 October 2012
Accepted 12 October 2012

Keywords:
Rhenium
Carbonyl
Crystal structures
Sulfonamide
Fluorescein
Metal conjugate

ABSTRACT

The new pyridine-2-carboxaldehyde adduct, $Re(CO)_3(NC_6H_5C(O)H)Cl$ **1**, and previously reported complex $Re(CO)_3(NC_6H_5C(O)H)Br$ **2** react with aniline derivatives sulfanilamide or 4-aminofluorescein in methanol giving Schiff base conjugates $Re(CO)_3$(pyca-R)X (pyca = pyridinecarbaldehyde imine, X = Cl, Br), **3**–**6**. Pre-isolation of compounds **1** and **2** provides a convenient method for preparing conjugate complexes in addition to the known methods of ligand synthesis and one-pot reactions. All new compounds were completely characterized, and compound **1** and the sulfanilamide derivatives **3** and **4** were structurally elucidated by X-ray crystallography.

1. Introduction

The biological chemistry of organometallic rhenium compounds has attracted research interest in recent years [1–3]. Initially, the goal was to examine cold analogs of technetium-99m, which is the most commonly used nuclide in nuclear medicine with 50,000 clinical applications per day in the US [4]. The creation of a kit for the preparation of $^{99m}Tc(CO)_3(H_2O)_3^+$ [5], opened up the possibility of $^{99m}Tc(CO)_3^+$ radiopharmaceuticals [6]. As technetium has no stable nuclides, exploring the similar chemistry of its higher congener is a convenient method of testing new targeting strategies for researchers searching for target specific radiopharmaceuticals. More recently, the field has been expanded by the development of a carrier-free source of rhenium-188 (half-life of 17 h with $\beta^- = 2.1$ MeV) and the production of a clinically appropriate method for the preparation of $^{188}Re(CO)_3(H_2O)_3^+$ [7–9]. The possibility of creating a matched pair of radiopharmaceuticals—one for diagnosis and one for therapy—that would target the same location is an attractive goal for clinical medicine [10]. Similarly, d^6 rhenium compounds have been tested as *in vivo* luminescence agents. Many of the compounds examined for this purpose contain polypyridyl units or dyes as ligands [11–13].

We and others have frequently made use of Schiff base condensation reactions to create d^6 rhenium compounds with diimine-based bioconjugates formed by the reaction of pyridine-2-carboxaldehyde with amino acid esters [14,15], amino acids [16], peptides [17] or amino alcohols [18]. Reactions of $Re(CO)_3^+$ precursors and pyridine-2-carboxaldehyde with amino acid esters yielded discrete mononuclear complexes, $Re(CO)_3$(pyca-Xxx-OR)Cl (pyca = pyridinecarbaldehyde imine, Xxx = amino acid), while amino acids or peptides yielded C_2-symmetric dimers, $[Re(CO)_3$(pyca-Xxx-O)$]_2$ or complex structures with extended hydrogen bonding networks. After the application of a strong base, amino alcohol conjugates produced a dimetallacycle with a proton strongly bonded between the two alkoxo oxygen atoms.

These metal Schiff base compounds have typically been made in one-pot reactions [16], as the iminopyridine ligands are not easy to isolate and use in further reactions. With the report on the synthesis of **2**, a bidentate adduct of pyridine-2-carboxaldehyde, we began looking to explore this reagent to expand the scope of amines used to create d^6 rhenium Schiff base complexes. We chose to focus on examining the reactivity of **2** and its chloride analog with substituted anilines, inspired by the work of Miguel and co-workers [19].

* Corresponding authors.
E-mail address: rherrick@holycross.edu (R.S. Herrick).

0022-328X/$ – see front matter © 2012 Elsevier B.V. All rights reserved.
http://dx.doi.org/10.1016/j.jorganchem.2012.10.025

There has been a significant amount of work on the synthesis and characterization of N-phenyl-2-pyridylimino $Re(CO)_3$ complexes. Since the early 1980s, both the chloride and the bromide variants of the unsubstituted N-phenyl-2-pyridylimino compounds have been prepared, typically by first separately synthesizing the pyridyl imine followed by chelation to the metal ion [20–22]. Alternatively, one-pot methods can be used; we employed such a method to generate $Re(CO)_3$ complexes incorporating pyca-amino acid conjugates. Using the older method of pre-generating the pyridyl imine ligand, a variety of functional groups can be introduced on the phenyl ring, including alkyl groups [21,23,24], hydroxides [25], halides [26,27], additional phenyls [23,28], and crown ethers [29,30]. Miguel used compound **2** to not only generate the phenyl species, but also analogs with carboxylic acids and alkynes substituted on the phenyl ring [19,31].

For this study, we chose to prepare complexes prepared from sulfanilamide and 4-aminofluorescein. Sulfonamide compounds have found use as inhibitors of carbonic anhydrase, and thus have been used as therapeutics for glaucoma, hypertension, and for use as diuretics [32]. The discovery of isozymes of carbonic anhydrase that are overexpressed in certain tumors has also encouraged researchers to create new sulfonamide compounds with applications such as targeting by luminescence or γ-emission [33,34]. The publication of the crystal structure of carbonic anhydrase with the metal complex, $Cp^RRe(CO)_3$ (R = arylsulfonamide) bound to the zinc ion at the active site highlights the interest in this area [35,36]. Although 4-aminofluorescein is not fluorescent, the parent fluorescein molecule finds heavy use in cellular imaging, and the development of $Re(CO)_3^+$ based luminescent molecules has been a goal of many research groups [11–13]. We were curious whether incorporating the exocyclic amine of 4-aminofluorescein into a metal-bound diimine ligand would return the fluorescent properties of this chromophore.

In this report we present the reaction of sulfanilamide and 4-aminofluorescein with $Re(CO)_3(C_5H_4C(O)H)X$; X = Cl, Br (**1** and previously prepared **2**, respectively) to form new compounds **3**–**6** (see Scheme 1 for numbering of compounds). The structures of both sulfanilamide products, **3** and **4**, as well as **1**, were elucidated by X-ray crystallography. Compounds **5** and **6** each regained fluorescence intensity upon incorporation of the exocyclic amine into the rhenium-bound diimine. The new pyridine aldehyde complex **1** and all of the new pyridyl imine compounds were completely characterized.

2. Results and discussion

2.1. Syntheses

The synthesis of compound **2** using an extended reflux of the aldehyde and one equivalent of $Re(CO)_5Br$ in hexane was first reported by Miguel and co-workers [15]. We found that the synthesis also works well in toluene, producing pure product that can be isolated and stored as a reagent for later reactions. We also prepared the new compound **1** by this same method. Both complexes were prepared in yields of greater than 80%. Compounds **3**–**6** were prepared as orange solids by methanol reflux of the appropriate aldehyde complex with one equivalent of the amine. Sulfonamide derivatives **3** and **4** were obtained as pure compounds by slow evaporation of the reaction solution. Fluorescein conjugate compounds **5** and **6** were insoluble. After precipitating from the solution during the reaction, they were washed and dried. Single crystals of **1**, **3** and **4** were grown using either diffusion of hexane into a CH_2Cl_2 solution in the case of **1** or by slow evaporation of a methanol solution in the cases of **3** and **4**.

Preparations of all reported compounds are insensitive to the presence of atmospheric oxygen and water vapor. No special precautions were taken in these syntheses.

2.2. Description of crystal structures

The structures of compounds **1**, **3** and **4** were elucidated by single crystal X-ray diffraction. The molecular structures are shown in Figs. 1 and 2. Crystal data and experimental details are listed in Table 1. Table 2 lists some of the key bond lengths and angles in these complexes. All of the complexes have slightly distorted octahedral geometries, with the three carbonyls arranged in a facial configuration as expected for d^6 $Re(CO)_3$ compounds.

Compound **1** is nearly isostructural to **2**. The aldehyde and pyridine units form a planar bidentate chelate to the metal ion with a Re–N distance of 2.177(5) Å and a Re–O distance of 2.172(4) Å. The carbonyls adopt the expected facial geometry and exhibit standard bond lengths and angles for $Re(CO)_3$ compounds. The Re–Cl bond length (2.4792(17) Å) is typical for the $Re(CO)_3Cl$ compounds, such as those that we previously observed in the similarly structured oxime and dioxime complexes [37]. The C–O bond length of the aldehyde (1.241(7) Å) is slightly lengthened versus that seen in free pyridine aldehydes, indicative of back

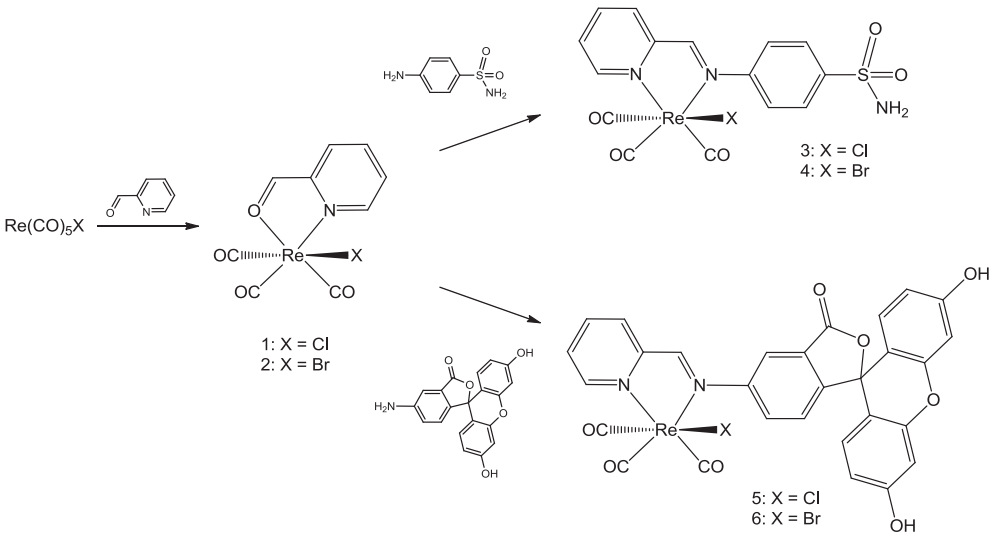

Scheme 1. General reaction scheme and numbering system for compounds **1**–**6**.

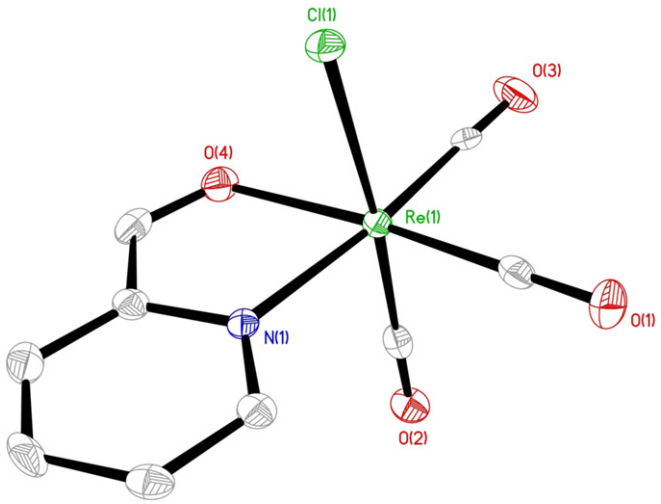

Fig. 1. The structure of compound **1** with 35% thermal ellipsoids. Hydrogen atoms have been omitted for clarity.

bonding to the carbonyl oxygen. Miguel and co-workers see a similar C–O bond length of 1.223(8) Å for the bromide derivative [15].

Complexes **3** and **4** were each characterized by single crystal X-ray crystallography; the molecular structures both of these compounds are shown in Fig. 2. Compounds **3** and **4** maintain a planar bidentate ligand, a facial set of carbonyls and a Re–X bond perpendicular to the pyridyl imine chelate. The bond distances and angles around the rhenium metal centers in these two compounds are as expected for pyridyl imine $Re(CO)_3$ compounds. The imine bonds in **3** and **4** are longer (1.284(10) and 1.303(9) Å, respectively) than the corresponding aldehyde carbonyl bonds in **1** and **2**, due to the increased π back bonding to the diimine unit. The two compounds also exhibit different orientations of the phenyl ring of the sulfanilamide group; in compound **4**, the plane of the ring phenyl ring is out of the plane of the pyridyl imine chelate by ~41°, whereas in compound **3** the two planes are more orthogonal, with an angle of ~76°. Compounds **5** and **6** did not produce single crystals despite numerous attempts and were characterized by spectroscopic methods. All CO bond lengths fall within the normal range as expected for $Re(CO)_3$ compounds.

In compound **3**, we were able to refine on a solvent methanol in the crystal structure. This methanol engages in a hydrogen bonding interaction with the sulfonamide nitrogen with a O···N distance of ~2.85 Å. In addition, there is a second hydrogen bond observed between the sulfonamide NH_2 group and the rhenium-bound chloride of a neighboring compound. This second interaction has an N···Cl distance of ~3.26 Å. For compound **4**, the solvent methanol was modeled as a diffuse contribution to the difference map without assigning specific atom positions using the SQUEEZE program, so we were not able to discern any solid state hydrogen bonding interactions between **4** and solvent. However, due to the alternate packing structure in **4**, no hydrogen bonding between the sulfonamide NH_2 group and the metal-bound bromide is observed. We speculate that the differences in packing between the two structures (and the observation of two different space groups for essentially isostructural molecules) may result from the presence of the NH–Cl hydrogen bond in **3** and the absence of an analogous NH–Br interaction in **4.**

2.3. Spectroscopic characterization

IR spectra of the new compounds displayed two metal carbonyl bands between about 2010 and 1840 cm^{-1}. This is consistent with vibrations analogous to a_1 and e modes resulting from a pseudo-C_{3v} symmetry for the compounds. Compound **1** also exhibits a carbonyl stretch from the metal-bound aldehyde unit at 1662 cm^{-1}. This value is significantly altered from that of free pyridine-2-carboxyaldehyde, which appears at 1730 cm^{-1} [38].

The NMR spectra of each compound were consistent with the observed structures for these complexes. The spectrum of compound **1** provided important information confirming its identity. The ^1H NMR spectrum showed a singlet at 9.98 ppm that is diagnostic of the aldehyde proton, and pyridine protons show up in expected locations. The ^{13}C NMR spectrum showed a peak at 192.6 ppm—appearing in the middle of the metal carbonyl resonances—due to the aldehyde carbon atom. As expected, the ^1H and ^{13}C spectra of **1** closely match the spectra of **2**. The ^1H and ^{13}C NMR spectra of compounds **3** and **4** displayed peaks due to the amide and phenyl groups in the regions expected. Spectra for each compound show peaks for the pyridine and imine functional groups in the expected regions. As typically observed for similar metal complexes, the protons closest to the metal are shifted downfield more than their neighbors.

As the structures of compounds **5** and **6** could not be elucidated by X-ray crystallography, NMR spectra were carefully analyzed and mass spectrometry was employed to verify their identities. In

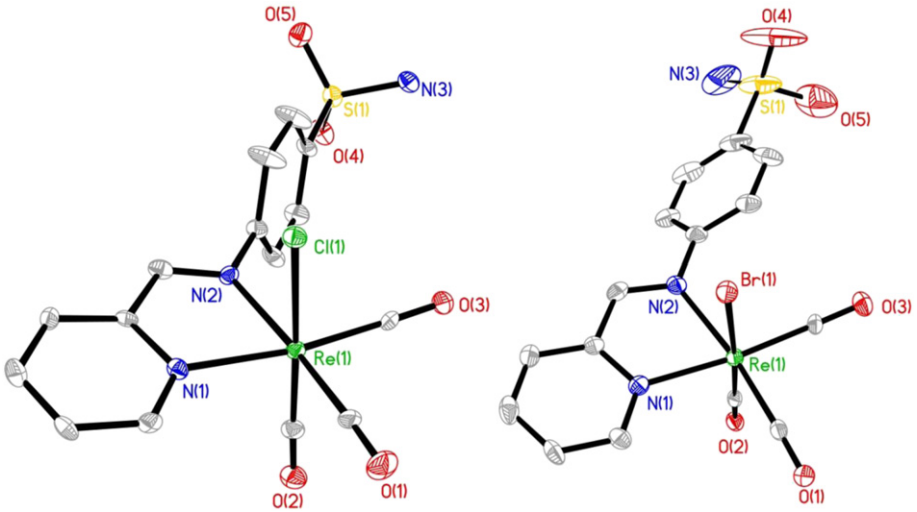

Fig. 2. The structures of **3** (left) and **4** (right) with 35% thermal ellipsoids. Hydrogen atoms have been omitted for clarity.

Table 1
X-ray data collection and structure parameters for compounds **1**, **3**, and **4**. Measurements were made at 100(2)K using Mo K_α radiation ($\lambda = 0.71073$ Å).

Compound	**1**	**3**	**4**
Empirical formula	$C_9H_5ClNO_4Re$	$C_{16}H_{10}ClN_3O_6ReS$	$C_{15}H_{11}BrN_3O_5ReS$
Formula weight	412.79	593.98	611.44
Crystal system	Monoclinic	Monoclinic	Rhombohedral
Space group	P2(1)/c	C2/c	R-3
Unit cell dimensions	$a = 10.533(5)$ Å	$a = 25.649(13)$ Å	$a = 36.910(5)$ Å
	$\alpha = 90°$	$\alpha = 90°$	$\alpha = 90°$
	$b = 8.880(4)$ Å	$b = 10.666(6)$ Å	$b = 36.910(5)$ Å
	$\beta = 91.130(7)°$	$\beta = 91.639(6)°$	$\beta = 90°$
	$c = 11.506(5)$ Å	$c = 14.356(8)$ Å	$c = 8.0828(10)$ Å
	$\gamma = 90°$	$\gamma = 90°$	$\gamma = 120°$
Volume	1076.0(8) $Å^3$	3926(4) $Å^3$	9536(2) $Å^3$
Z	4	8	18
Density (calculated)	2.548 mg/m^3	2.010 mg/m^3	1.916 mg/m^3
Absorption coefficient	11.537 mm^{-1}	6.471 mm^{-1}	7.745 mm^{-1}
F(000)	760	2264	5184
Crystal size	0.17 × 0.14 × 0.09 mm^3	0.10 × 0.10 × 0.03 mm^3	0.30 × 0.08 × 0.04 mm^3
Theta range for data collection	1.93°–26.99°	1.59°–27.57°	1.91°–27.52°
Index ranges	$-13 <= h <= 13$,	$-32 <= h <= 33$,	$-47 <= h <= 47$,
	$-11 <= k <= 11$,	$-13 <= k <= 13$,	$-47 <= k <= 47$,
	$-14 <= l <= 14$	$-18 <= l <= 18$	$-10 <= l <= 10$
Reflections collected	8689	15,759	26,228
Independent reflections	2352 [R(int) = 0.0582]	4418 [R(int) = 0.0755]	4851 [R(int) = 0.0550]
Completeness to theta	99.9%	97.1%	99.1%
Absorption correction	SADABS	SADABS	SADABS
Max. and min. transmission	0.4233 and 0.2445	0.8295 and 0.5639	0.7470 and 0.2047
Refinement method	Full-matrix least-squares on F^2	Full-matrix least-squares on F^2	Full-matrix least-squares on F^2
Data/restraints/parameters	2352/0/145	4418/0/256	4851/0/236
Goodness-of-fit on F^2	0.91	1.001	0.923
Final R indices [$I > 2$sigma(I)]	$R1 = 0.0294$, $wR2 = 0.0574$	$R1 = 0.0461$, $wR2 = 0.1012$	$R1 = 0.0402$, $wR2 = 0.1189$
R indices (all data)	$R1 = 0.0395$, $wR2 = 0.0585$	$R1 = 0.0614$, $wR2 = 0.1107$	$R1 = 0.0496$, $wR2 = 0.1274$
Largest diff. peak and hole	2.231 and −0.935 e $Å^{-3}$	1.863 and −2.189 e $Å^{-3}$	1.653 and −1.334 e $Å^{-3}$

Table 2
Selected bond lengths (Å) and bond angles (°) for **1**, **3**, and **4**.

	1	**3**	**4**
Bond lengths			
Re(1)–C(1)	1.896(7)	1.916(8)	1.926(7)
Re(1)–C(2)	1.903(6)	1.909(8)	1.922(6)
Re(1)–C(3)	1.908(7)	1.935(8)	1.918(6)
Re(1)–N(1)	2.177(5)	2.187(6)	2.170(5)
Re(1)–Cl(1)	2.4792(17)	2.499(2)	
Re(1)–Br(1)			2.6294(7)
Re(1)–O(4)	2.172(4)		
Re(1)–N(2)		2.161(6)	2.187(6)
C(9)–O(4)	1.241(7)		
C(9)–N(2)		1.278(10)	1.303(9)
Bond angles			
C(1)–Re(1)–C(3)	90.1(3)	90.1(3)	89.1(3)
C(1)–Re(1)–C(2)	89.7(2)	88.1(3)	86.9(3)
C(3)–Re(1)–C(2)	87.5(2)	88.9(3)	90.3(3)
C(3)–Re(1)–O(4)	97.6(2)		
C(2)–Re(1)–O(4)	91.52(19)		
C(3)–Re(1)–N(2)		96.7(3)	91.7(2)
C(2)–Re(1)–N(2)		97.2(3)	100.8(2)
C(2)–Re(1)–N(1)	92.4(2)	94.2(3)	94.3(2)
C(1)–Re(1)–N(1)	97.4(2)	98.1(3)	97.5(2)
O(4)–Re(1)–N(1)	74.91(17)		
N(2)–Re(1)–N(1)		74.9(2)	74.8(2)
C(1)–Re(1)–Cl(1)	95.40(18)	92.4(2)	
C(3)–Re(1)–Cl(1)	94.31(18)	93.1(2)	
O(4)–Re(1)–Cl(1)	83.17(11)		
N(1)–Re(1)–Cl(1)	85.15(12)	83.76(16)	
N(2)–Re(1)–Cl(1)		82.08(17)	
C(1)–Re(1)–Br(1)			93.74(19)
C(3)–Re(1)–Br(1)			92.39(19)
N(1)–Re(1)–Br(1)			82.77(14)
N(2)–Re(1)–Br(1)			85.19(14)

addition to the expected peaks for the pyridine and imine groups in both the ^1H and ^{13}C NMR spectra, the compounds showed the appropriate number of peaks in proper locations, consistent with a modified 4-aminofluorescein moiety. In addition, ^{13}C NMR data established the formation of compound **5** and **6** as observed by the conversion of the aldehyde (C(H)═O) to an imine via the reaction with 4-fluoresceinamine, as shown in Fig. 3. The aldehyde carbon atom shifts from 192.6 ppm (top spectrum) in **1** to 159.7 ppm in **5**. Compound **6** shows a similar resonance for its imine carbon at 160.2 ppm. Comparison of the actual sample isotope pattern recorded for the mass spectra for **5** and **6** to the simulated (expected) isotope pattern (Fig. 4) confirms the identity of these compounds.

The UV–visible spectra for **5** and **6** were measured, and as expected the spectra are dominated by fluorescein-based transitions. The spectra of both compounds along with that of 4-aminoflurescein are shown in Fig. 5. We determined the extinction coefficients for the primary absorption peak to be 7.96×10^4 M^{-1} cm^{-1} at 500 nm for compound **5** and 6.54×10^4 M^{-1} cm^{-1} at 497 nm for compound **6**. These molar absorptivities are in the same range as that seen in unmodified 5-aminoflurescein. Compounds **5** and **6** each fluoresce when the absorption maxima at 500 nm and 497 nm, respectively, are irradiated. Fig. 6 shows the excitation and emission spectra of the two fluorescein conjugate complexes. The emission resembles that of normal fluorescein in both profile and Stokes shift. When compared to normal fluorescein, which has a quantum yield of 0.79 [39], the quantum yield of emission is significantly reduced, measuring ~0.038 for both compounds **5** and **6**. The reduction in quantum yield can be directly attributed to the heavy atom effect due to the close proximity of the rhenium and the halide. However, the emission of these two compounds is increased relative to that of 4-aminofluorescein, which is non-emissive. The formation of the Schiff base and metal coordination of the amine nitrogen of 4-

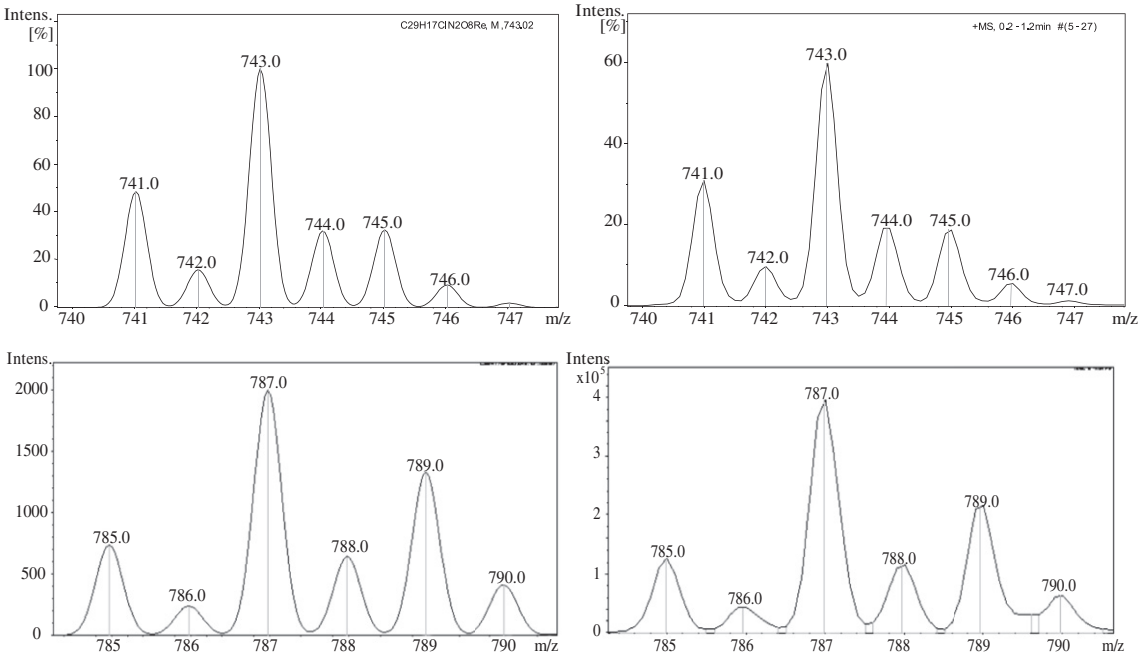

Fig. 3. Top: predicted (left) and observed (right) ESI MS of **5**. Bottom: predicted (left) and observed (right) ESI MS of **6**.

aminofluorescein restores the fluorescence; the restoration of fluorescence upon metal binding of exocyclic amines is a well-known property of fluorescein-based dyes [40–43].

2.4. Conclusions

We have found that pyridine aldehyde-bound rhenium(I) carbonyls can be used to readily generate biologically relevant conjugate complexes. The metal-bound aldehyde readily reacts with amines such as anilines to afford imines. In the current study, we have successfully generated conjugates incorporating sulfanilamide and 4-aminofluorescein, producing the corresponding $Re(CO)_3$(pyca-R)X compound with the pyridyl imine covalently linked to the desired biological molecule. Our work continues with these compounds and similar biologically relevant conjugates of $Re(CO)_3$.

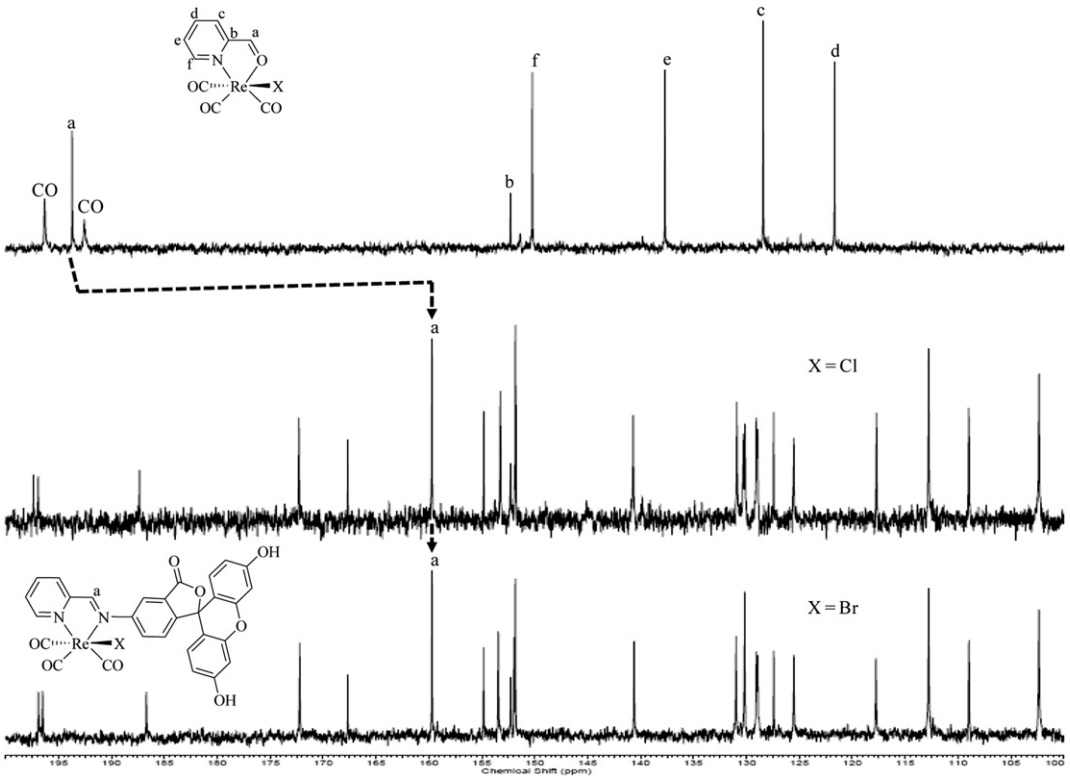

Fig. 4. ^{13}C NMR spectra for **1** (top), **5** (middle) and **6** (bottom). The arrow shows the shift of the aldehyde carbon resonance for **1** relative to the imine carbon resonances for **5** and **6**.

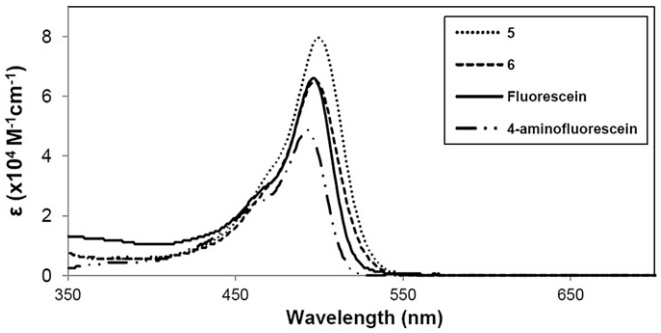

Fig. 5. UV–visible absorption spectra for **5**, **6**, fluorescein, and 4-aminofluorescein.

3. Experimental

3.1. Materials and methods

All reagents were purchased from Strem, Acros Organics or Sigma–Aldrich and used as received. NMR spectroscopy was performed with Varian VXR 300 MHz and Varian 500 MHz NMR instruments. Elemental analyses were carried out at the School of Chemical Sciences Microanalytical Laboratory at the University of Illinois at Urbana-Champaign. Mass spectrometric analyses were carried out at the Mass Spectrometry and Proteomics Facility at the Ohio State University in Columbus, OH or at the University of Akron in Akron, OH. IR spectra were recorded on a Nicolet Series II Magna-IR 750 spectrometer. UV–visible spectroscopy was carried out on a Hitachi U-3010 spectrometer. Fluorescence measurements were made on a Horiba Jobin Yvon FluoroMax-4 spectrofluorometer. Fluorescence quantum yield measurements were made relative to normal fluorescein as a standard [44].

3.2. Synthesis of **1** and **2**

Compound **1** and previously reported **2** [15] were prepared by similar methods. No special precautions were taken as the synthetic procedure and the resulting products are not air or moisture sensitive. In a typical reaction, $Re(CO)_5Cl$ (0.200 g, 0.552 mmol) was mixed with one equivalent of pyridine-2-carboxaldehyde (0.0590 g, 0.552 mmol) and 15 mL of toluene. The mixture was then heated to reflux for 24 h, slowly causing the solution to turn orange–red. Upon completion of the reaction, a red product was collected by filtration. The product was washed with diethyl ether and dried. Crystals suitable for X-ray diffraction were grown by vapor diffusion of pentane into a CH_2Cl_2 solution of the compound.

Compound **1**: Yield 132 mg, 58%. ^{1}H NMR (d_6-DMSO, δ ppm): 9.98 (s, 1H, (C*H*O)), 8.83 (d, J = 4.2 Hz, 1H, *H* on py), 8.06 (t, J = 7.5 Hz, 1H, *H* on py), 7.94 (d, J = 7.5 Hz, 1H, *H* on py), 7.71(m, 1H, *H* on py). ^{13}C NMR (d_6-DMSO, δ ppm) 196.3, 193.7, 192.6, 152.30, 150.3, 137.7, 128.4, 121.68. ESI MS (positive ion) $[M - Cl]^+$: 377.9 m/z Calc. 377.35 m/z; CHN Anal. Calc. for $ReC_9H_5O_4NCl$: C, 26.19; H, 1.22; N, 3.39. Found: C, 25.87; H, 0.99; N, 3.20. IR (CO stretch, cm^{-1}): 2023(s), 1892(s), 1662(m).

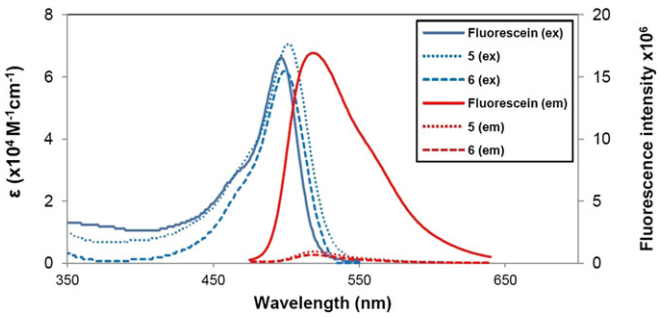

Fig. 6. Excitation and emission spectra for **5**, **6**, and fluorescein.

3.3. Synthesis of **3** and **4**

Preparation of **3**: **1** (0.050 g, 0.12 mmol) was mixed with one equivalent of sulfanilamide (0.020 g, 0.12 mmol) and 10 mL methanol was then added to the flask. The mixture was heated to reflux. During the 6 h reflux, the red solution turned to a dark orange–red color. The solution volume was decreased by slow evaporation and an orange solid was collected by filtration. The product was washed with diethyl ether and dried. Crystals suitable for characterization by X-ray diffraction were formed by slow evaporation of methanol.

Compound **3**: Yield 56 mg, 82%. ^{1}H NMR (d_6-DMSO, δ ppm): 9.41 (s, 1H, N=C*H*), 9.10 (d, J = 5.5 Hz, 1H, *H* on py), 8.39 (d, J = 3.5 Hz, 1H, *H* on py), 8.03 (m, 2H, *H* on C_6H_4), 7.88 (m, 2H, *H* on py), 7.72 (d, J = 9.0 Hz, 2H, H on C_6H_4), 7.51 (s, 2H, NH_2). ^{13}C NMR (d_6-DMSO, δ ppm) 197.9, 197.3, 187.7, 171.9, 155.3, 153.7, 153.1, 144.7, 141.1, 131.3, 130.7, 127.6, 123.4, 112.9, 105.0. ESI MS (positive ion) $[M + Na]^+$: 589.9 m/z Calc. 589.9 m/z; CHN Anal. Calc. for $ReC_{15}H_{11}O_5N_3SCl$: C, 31.78; H, 1.96; N, 7.41. Found: C, 31.74; H, 1.99; N, 7.29. IR (CO stretch, cm^{-1}): 2021(m), 1895(s).

Preparation of **4**: This compound was synthesized via an identical procedure as **3**. Crystals for structural analysis were grown by slow evaporation from methanol.

Compound **4**: Yield 57 mg, 85%. ^{1}H NMR (d_6-DMSO, δ ppm): 9.39 (s, 1H, N=C*H*), 9.13 (d, J = 5.5 Hz, 1H, *H* on py), 8.39 (m, 1H, *H* on py), 8.03 (d, J = 7 Hz, 2H, *H* on C_6H_4), 7.87 (m, 2H, *H* on py), 7.73 (d, J = 5 Hz, 2H, *H* on C_6H_4), 7.51 (s, 2H, NH_2). ^{13}C NMR (d_6-DMSO, δ ppm) 197.4, 196.9, 187.1, 171.8, 155.3, 153.9, 153.21, 144.7, 141.0, 131.4, 130.6, 127,8, 127.6, 123.4, 112.9 ESI MS (positive ion): $[M + Na]^+$: 633.9 m/z Calc. 634.4 m/z; CHN Anal. Calc. for $ReC_{15}H_{11}O_5N_3SBr$: C, 29.46; H, 1.81; N, 6.87. Found: C, 29.01; H, 1.64; N, 6.66. IR (CO stretch, cm^{-1}): 2023(m), 1897(s).

3.4. Synthesis of **5** and **6**

Preparation of **5**: Compound **1** (50 mg, 0.12 mmol) was mixed with one equivalent of 4-aminofluorescein (42 mg, 0.12 mmol) and 25 mL methanol was added to the flask. The mixture was heated to reflux. During the 6 h reflux, an orange precipitate formed which was collected by filtration. The product was washed with cold methanol and dried.

Compound **5**: Yield 81 mg, 91%. ^{1}H NMR (d_6-DMSO, δ ppm): 10.23 (br s, 2H O*H*), 9.47 (s, 1H, N=C–*H*), 9.10 (d, J = 5.6 Hz, 1H, *H* on py), 8.39 (m, 2H, *H* on Ar), 8.14 (d, 2.0 Hz, 1H, *H* on Ar), 7.89 (m, 1H *H* on py), 7.72 (m, 1H, *H* on py), 7.51 (d, J = 8.1 Hz, 1H, *H* on Ar), 6.70 (m, 2H, *H* on Ar), 6.64 (d, J = 8.1 Hz, 1H, *H* on Ar), 6.63 (m, 3H, *H* on Ar). ^{13}C NMR (d_6-DMSO, δ ppm) 197.8, 197.4, 187.8, 172.7, 168.1, 160.2, 155.3, 153.7, 152.8, 152.3, 141.2, 131.4, 130.8, 130.6, 129.5, 129.4, 127.9, 126.0, 118.2, 113.2, 109.6, 102.8, 83.6. ESI MS (positive ion) (M + H): 743.0 m/z Calc. 743.1 m/z; CHN Anal. Calc. for $ReC_{29}H_{16}O_8N_2Cl\cdot 0.5H_2O$: C, 46.37; H, 2.18; N, 3.73. Found: C, 46.16; H, 1.96; N, 3.70. IR (CO stretch, cm^{-1}): 2017(m), 1920(s), 1862(s).

Preparation of **6**: This compound was synthesized via an identical procedure as **5**.

Compound **6**: Yield 76 mg, 89%. ^{1}H NMR (d_6-DMSO, δ ppm): 10.19 (br s, 2H O*H*), 9.47 (s, 1H, N=C–*H*), 9.12 (d, J = 5.6 Hz, 1H, *H* on py), 8.38 (m, 2H, *H* on Ar), 8.14 (d, 2.0 Hz, 1H, *H* on Ar), 8.00 (m, 1H *H* on py), 7.85 (m, 1H, *H* on py), 7.53 (d, J = 8.1 Hz, 1H, *H* on Ar), 6.67 (m, 2H, *H* on Ar), 6.63 (d, J = 8.1 Hz, 1H, *H* on Ar), 6.60 (m, 3H, *H*

on Ar). ^{13}C NMR (d_6-DMSO, δ ppm) 196. 9, 196.10, 186.7, 172.2, 167.7, 159.7, 154.8, 153.4, 152.3, 152.0, 151.8, 140.6, 131.0, 130.2, 129.1, 128.9, 127.4, 125.5, 117.8, 112.8, 109.0, 102.4, 83.6. ESI MS (positive ion) (M + H): 787.0 *m*/*z* Calc. 787.5 *m*/*z*; CHN Anal. Calc. for $ReC_{29}H_{16}O_8N_2Br\cdot 0.5H_2O$: C, 43.78; H, 2.15; N, 3.52. Found: C, 43.75; H, 1.84; N, 3.46; IR (CO stretch, cm^{-1}): 2018(m), 1927(s), 1868(s).

3.5. X-ray structure determination of **1**, **3** and **4**

X-ray intensity data were measured at 100 K (Bruker KYRO-FLEX) on a Bruker SMART APEX CCD-based X-ray diffractometer system equipped with a Mo-target X-ray tube (λ = 0.71073 Å) operated at 2000 W power. The crystals were mounted on a cryoloop using Paratone N-Exxon oil and placed under a stream of nitrogen at 100 K. The detector was placed at a distance of 5.009 cm from the crystals. The data were corrected for absorption with the SADABS program. The structures were refined using the Bruker SHELXTL Software Package (Version 6.1), and were solved using direct methods until the final anisotropic full-matrix, least-squares refinement of F^2 converged [45]. Crystal data and structure refinement parameters are shown in Table 1.

Acknowledgments

RSH would like to thank the Research Corporation (CC6663/6616) and the Petroleum Research Fund (51085-UR3) for financial support of this research. CJZ acknowledges the National Institutes of Health (R15 GM083322) for funds used in this work.

Appendix A. Supplementary material

CCDC 895955–895957 contain the supplementary crystallographic data for this paper. These data can be obtained free of charge from The Cambridge Crystallographic Data Centre via www.ccdc.cam.ac.uk/data_request/cif.

References

[1] R.S. Herrick, New Developments in Organometallic Research, Nova Science Publishers, Inc., New York, 2006, pp. 117–149.
[2] R. Schibli, P.A. Schubiger, Eur. J. Nucl. Med. Mol. Imaging 29 (2002) 1529–1542.
[3] M. Bartholomae, J. Valliant, K.P. Maresca, J. Babich, J. Zubieta Chem. Commun. (2009) 493–512.
[4] I. Amato, Chem. Eng. News 87 (2009) 58–64.
[5] R. Alberto, K. Ortner, N. Wheatley, R. Schibli, A.P. Schubiger, J. Am. Chem. Soc. 123 (2001) 3135–3136.
[6] S. Liu, Chem. Soc. Rev. 33 (2004) 445–461.
[7] P. Kozminski, E. Gniazdowska, L. Fuks, S. Kowalska, Appl. Radiat. Isot. 69 (2011) 436–442.
[8] L. Fuks, E. Gniazdowska, P. Kozminski, Polyhedron 29 (2010) 634–638.
[9] R. Schibli, R. Schwarzbach, R. Alberto, K. Ortner, H. Schmalle, C. Dumas, A. Egli, P.A. Schubiger, Bioconjug. Chem. 13 (2002) 750–756.
[10] R. Alberto, in: E. Alessio (Ed.), Bioinorganic Medicinal Chemistry, Wiley-VCH, Weinheim, 2011, pp. 253–282.
[11] K.K.-W. Lo, K.Y. Zhang, S.P.-Y. Li, Eur. J. Inorg. Chem. (2011) 3551–3568.
[12] R.G. Balasingham, M.P. Coogan, F.L. Thorp-Greenwood, Dalton Trans. 40 (2011) 11663–11674.
[13] K.K.-W. Lo, M.-W. Louie, K.Y. Zhang, Coord. Chem. Rev. 254 (2010) 2603–2622.
[14] R.S. Herrick, I. Wrona, N. McMicken, G. Jones, C.J. Ziegler, J. Shaw, J. Organomet. Chem. 689 (2004) 4848–4855.
[15] C.M. Alvarez, R. Garcia-Rodriguez, D. Miguel, Dalton Trans. (2007) 3546–3554.
[16] H. Qayyum, R.S. Herrick, C.J. Ziegler, Dalton Trans. 40 (2011) 7442–7445.
[17] C.M. Alvarez, R. Garcia-Rodriguez, D. Miguel, Inorg. Chem. 51 (2012) 2984–2996.
[18] C.M. Alvarez, R. Garcia-Rodriguez, J.M. Martin-Alvarez, D. Miguel, J.A. Turiel, Inorg. Chem. 51 (2012) 3938–3940.
[19] L.A. Garcia-Escudero, D. Miguel, J.A. Turiel, J. Organomet. Chem. 691 (2006) 3434–3444.
[20] R.W. Balk, D.J. Stufkens, A. Oskam, J. Chem. Soc. Dalton Trans. (1981) 1124–1133.
[21] M.W. Kokkes, T.L. Snoeck, D.J. Stufkens, A. Oskam, M. Christophersen, C.H. Stam, J. Mol. Struct. 131 (1985) 11–29.
[22] R.N. Dominey, B. Hauser, J. Hubbard, J. Dunham, Inorg. Chem. 30 (1991) 4754–4758.
[23] V.W.-W. Yam, Y. Yang, J. Zhang, B.W.-K. Chu, N. Zhu, Organometallics 20 (2001) 4911–4918.
[24] V.W.-W. Yam, K.-Z. Wang, C.-R. Wang, Y. Yang, K.-K. Cheung, Organometallics 17 (1998) 2440–2446.
[25] W. Liu, K. Heinze, 39 (2010) 9554–9564.
[26] M. Khalaj, S. Dehghanpour, R. Aleeshah, A. Mahmoudi, Acta Crystallogr. Sect. E: Struct. Rep. Online E66 (2010) m1647.
[27] S. Dehghanpour, A. Mahmoudi, Acta Crystallogr. Sect. E: Struct. Rep. Online E66 (2010) m1335.
[28] J. Zhang, B.W.-K. Chu, N. Zhu, V.W.-W. Yam, Organometallics 26 (2007) 5423–5429.
[29] K.M.-C. Wong, W.-P. Li, K.-K. Cheung, V.W.-W. Yam, New J. Chem. 29 (2005) 165–172.
[30] V.W.-W. Yam, K.M.-C. Wong, V.W.-M. Lee, K.K.-W. Lo, K.-K. Cheung, Organometallics 14 (1995) 4034–4036.
[31] C.M. Alvarez, R. Garcia-Rodriguez, D. Miguel, J. Organomet. Chem. 692 (2007) 5717–5726.
[32] C.T. Supuran, J.C. Scozzafava, Carbonic Anhydrase: Its Inhibitors and Activators, CRC Press, Boca Raton, 2004.
[33] O.O. Guler, S.G. De, C.T. Supuran, Curr. Med. Chem. 17 (2010) 1516–1526.
[34] J.-Y. Winum, M. Rami, A. Scozzafava, J.-L. Montero, C. Supuran, Med. Res. Rev. 28 (2008) 445–463.
[35] D. Can, B. Spingler, P. Schmutz, F. Mendes, P. Raposinho, C. Fernandes, F. Carta, A. Innocenti, I. Santos, C.T. Supuran, R. Alberto, Angew. Chem. Int. Ed. 51 (2012) 3354–3357.
[36] V. Akurathi, L. Dubois, N.G. Lieuwes, S.K. Chitneni, B.J. Cleynhens, D. Vullo, C.T. Supuran, A.M. Verbruggen, P. Lambin, G.M. Bormans, Nucl. Med. Biol. 37 (2010) 557–564.
[37] R. Costa, N. Barone, C. Gorczycka, E.F. Powers, W. Cupelo, J. Lopez, R.S. Herrick, C.J. Ziegler, J. Organomet. Chem. 694 (2009) 2163–2170.
[38] AIST: Integrated Spectral Database System of Organic Compounds. (Data were obtained from the National Institute of Advanced Industrial Science and Technology (Japan).)
[39] R.E. Kellogg, R.G. Bennett, J. Chem. Phys. 41 (1964) 3042–3045.
[40] A. Bencini, V. Lippolis, Coord. Chem. Rev. 256 (2012) 149–169.
[41] J. Wu, W. Liu, J. Ge, H. Zhang, P. Wang, Chem. Soc. Rev. 40 (2011) 3483–3495.
[42] M.H. Lim, S.J. Lippard, Acc. Chem. Res. 40 (2007) 41–51.
[43] L. Fabbrizzi, M. Licchelli, P. Pallavicini, L. Parodi, A. Taglietti, Perspect. Supramol. Chem. 5 (1999) 93–134.
[44] A.T.R. Williams, S.A. Winfield, J.N. Miller, Analyst 108 (1983) 1067.
[45] G.M. Sheldrick, Crystallographic Software Package. Version 6.10, Bruker-AXS, Madison, WI, 2000.